Hindawi
Journal of Chemistry
Volume 2017, Article ID 8545690, 7 pages
https://doi.org/10.1155/2017/8545690

Research Article

TiO_2/Pt/TiO_2 Sandwich Nanostructures: Towards Alcohol Sensing and UV Irradiation-Assisted Recovery

Rungroj Maolanon,[1,2] Winadda Wongwiriyapan,[1,3] and Sirapat Pratontep[1,3]

[1] *College of Nanotechnology, King Mongkut's Institute of Technology Ladkrabang, Chalongkrung Rd., Ladkrabang, Bangkok 10520, Thailand*
[2] *National Nanotechnology Center (NANOTEC), NSTDA, Thailand Science Park, Pathum Thani 12120, Thailand*
[3] *Nanotec-KMITL Center of Excellence on Nanoelectronics Device, Bangkok 10520, Thailand*

Correspondence should be addressed to Winadda Wongwiriyapan; winadda.wo@kmitl.ac.th

Received 9 June 2017; Revised 6 August 2017; Accepted 21 August 2017; Published 25 September 2017

Academic Editor: Łukasz Laskowski

The TiO_2/Pt/TiO_2 sandwich nanostructures were synthesized by RF magnetron sputtering and demonstrated as an alcohol sensor at room-temperature operation with a fast recovery by UV irradiation. The TiO_2/Pt/TiO_2 layers on SiO_2/Si substrate were confirmed by Auger electron spectroscopy with the interdiffusion of each layer. The TiO_2/Pt/TiO_2 layers on printed circuit board show the superior sensor response to alcohol in terms of the sensitivity and stability compared to the nonsandwich structure, that is, the only Pt layer or the TiO_2/Pt structures. Moreover, the recovery time of the TiO_2/Pt/TiO_2 was improved by UV irradiation-assisted recovery. The optimum TiO_2/Pt/TiO_2 with thicknesses of the undermost TiO_2 layer, a Pt layer, and the topmost TiO_2 layer being 50 nm, 6 nm, and 5 nm, respectively, showed the highest response to ethanol down to 10 ppm. Additionally, TiO_2/Pt/TiO_2 shows an excellent sensing stability and exhibits different sensing selectivity among ethanol, methanol, and 2-propanol. The sensing mechanism could be attributed to the change of Pt work function during vapor adsorption. The TiO_2 layer plays an important role in UV-assisted recovery by photocatalytic activity and the topmost TiO_2 acts as protective layer for Pt.

1. Introduction

Gas sensor plays an important role in gas detection and monitoring in many industrial or domestic activities. During the past few decades, gas sensor has been extensively developed, especially the case for application in monitoring automotive exhaust gases and air quality. Gas sensor has also become increasingly important in the detection of volatile organic compounds (VOCs) in the chemical industry, food industry, agriculture, and medical and indoor air quality control. The resistive gas sensors based on metal oxide and the change of the resistance after exposure to the reducing or oxidizing gas gain the great interest due to its numerous advantages such as low cost, easy production, compact size, and real-time operation [1, 2]. However, the performance of the resistive gas sensors is significantly influenced by the morphology and structure of sensing materials, resulting in a great obstacle for gas sensors based on bulk materials or dense films to achieve highly sensitive properties. Moreover, the metal oxide gas sensors are activated by heat from microheater, generally working at a temperature beyond 200°C, which limits their applications to plastic substrates, flammable gases, and some sensing materials which are changed with the factors of high temperature [3–7]. On the contrary, traditional analytical instruments such as mass spectrometer, nuclear magnetic resonance spectroscopy, and chromatography show high sensitivities but are expensive, complex, large in size, and difficult for real-time analysis. However, recent advances in nanotechnology have produced novel classes of nanostructured materials with enhanced gas sensing properties providing the opportunity to dramatically increase the performance of gas sensor.

The nanostructured materials, such as nanoparticle, nanowire, nanorod, and nanotube have demonstrated excellent sensing performance compared to conventional thin films [8–20]. The high selectivity of the sensors has been

improved by surface modification with noble metals such as Pt and Pd [21, 22]. To enhance stability of gas sensor, for example, in the system of carbon nanotube based sensor, metal oxide coating layer was used as a protective layer for highly stable and sensitive gas sensor [23, 24]. Moreover, heating or ultraviolet irradiation is an effective way to improve the fast recovery of the sensor using thermal energy or photoexcited plasmons for molecule desorption, respectively [20, 25, 26]. In terms of fabrication cost, it is desirable to achieve the high performance sensor based on the standard semiconductor technology without using advanced lithography methods. Thus, the development of the novel gas sensor with high performance using the existing process technology is a challenge for researcher.

Titanium dioxide (TiO_2) is known as the most extensively studied photocatalyst due to its excellent photocatalytic oxidation property, stability, low cost, and nontoxicity. TiO_2 with a transition metal functionalization such as Fe, Ni, Cu, Co, Ag, Au, and Pt shows a potential use in detection of toxic gases and VOCs [27–35] at the lower operation temperature through effective improvements of interaction between TiO_2 surface and the gas molecules. Moreover, taking an advantage of photocatalytic oxidation of TiO_2, the VOCs could be removed by photocatalytic degradation under UV light irradiation, affording the fast sensor recovery. However, these sensors still suffer with the elevated temperature operation and stability issues.

In this study, novel sensor based on TiO_2/Pt/TiO_2 sandwiched nanostructures with UV irradiation-assisted recovery was proposed for alcohol sensing at room temperature. Each layer was deposited by RF magnetron sputtering on printed circuit board (PCB) with interdigitated electrodes which is much cheaper and more flexible than Si substrate.

2. Materials and Methods

2.1. Fabrication of Gas Sensor Based on TiO_2-Pt-TiO_2 Sandwich Nanostructures. A printed circuit board (PCB) consisting of an interdigitated Cu/Au electrode was used as the sensor platform with a gap of 250 μm and a sensing area of 8×12 mm^2. The schematic view of the PCB structure is shown in Figure 1(a). The gas sensor materials consist of the undermost TiO_2, Pt, and the topmost TiO_2 layers with thicknesses of 50 nm, 6 nm, and 5 nm, respectively (TiO_2/Pt/TiO_2). The TiO_2 layer and the Pt layer were deposited by the RF magnetron sputtering (OERLIKON Leybold Vacuum, UNIVEX 35) and a DC ion sputtering (HITACHI, E-1010), respectively. The RF magnetron sputtering of TiO_2 layer was conducted by using rutile TiO_2 as a target under an Ar gas (99.999%) flow of 20 sccm, a deposition rate of 0.1 nm min^{-1}, and a power of 150 W. The total pressure in the deposition chamber was 6.6×10^{-3} mbar and the base pressure was 1.6×10^{-6} mbar. The substrates were rotated at 10 rpm and placed at a distance of 100 mm above the target surface. After a RF magnetron sputtering of the undermost TiO_2 layer, the sample was taken and immediately transferred for a Pt layer deposition to a DC ion sputtering machine, which is a typical machine for metal deposition in scanning electron microscopy observation. The DC ion sputtering of Pt layer was conducted by using Pt (purity 99.95%) as a target under a pressure of 7×10^{-2} mbar, a current of 15 mA, and a deposition rate of 6 nm min^{-1}. Finally, the sample was set back to a RF magnetron sputtering machine again for the topmost TiO_2 layer deposition using the same condition as the undermost TiO_2 layer. The schematic view of the TiO_2/Pt/TiO_2 sandwich nanostructures on the PCB substrate is shown in Figure 1(b). The TiO_2/Pt/TiO_2 sandwich nanostructures on the PCB substrate were further used for gas sensor measurement. Moreover, the TiO_2/Pt/TiO_2 sandwich nanostructures were synthesized on the SiO_2/Si substrate with the same condition for the elemental composition and the depth profile characterization. For internal structure characterization, the TiO_2/Pt/TiO_2 was directly deposited on Cu grid using the same deposition condition.

2.2. Morphology and Structural and Elemental Composition Characterizations of the TiO_2-Pt-TiO_2 Sandwich Nanostructures. The morphology of the PCB substrate was characterized by an environment scanning electron microscopy (E-SEM) (HITACHI; S-3400N). The internal structure of the synthesized TiO_2/Pt/TiO_2 on Cu grid was characterized by transmission electron microscope (TEM) (JEOL; 2100F). The elemental composition and the depth profile of the TiO_2/Pt/TiO_2 on SiO_2/Si were characterized by Auger electron spectroscopy (AES) (ULVAC; PHI-700) using an argon ion bombardment with an analytical area of 5×5 μm^2. The sputtering rate was approximately 1.25 nm min^{-1}. It should be noted that the Auger measurements were performed for the layers grown on a SiO_2/Si substrate instead of the layers on PCB due to the AES technical limitation in terms of charging effects in nonconducting samples.

2.3. Gas Sensor Measurement. Sensor responses of the TiO_2/Pt/TiO_2 layers to ethanol, methanol, and 2-propanol in a concentration of 10 to 100 ppm were measured in the static condition at room temperature by recording the electrical resistance using a multimeter (Fluke 45 dual display) during cycles of alternating supply of dry air and the test vapor. All chemicals are of analytical reagent grade from Fisher Scientific, UK. Dry air, which is mainly composed of approximately 80% nitrogen and 20% oxygen, was used as a baseline gas and a carrier gas. Firstly, sensors were placed in a stainless steel chamber (53.225l) equipped with an UV-LED light source with a wavelength of 365 nm under dry air for 50 s, followed by dropping of liquid of test vapor into the detection system and monitoring its resistance for 500 s. Finally, sensor was recovered by replacing with dry air and UV irradiation for 500 s. The schematic diagram of the test chamber is shown in Figure 2. The concentration of the test vapors was calculated from the volume of the liquid dropped into the sensor test chamber using a micropipette. The sensor response (S) is defined by $S = (R/R_0)$, whereas R and R_0 are the electrical resistance during the sensor test and the initial electrical resistance under the dry air of the sensor, respectively. Response time and recovery time are defined as the time taken by the sensor to reach 90% of its maximum

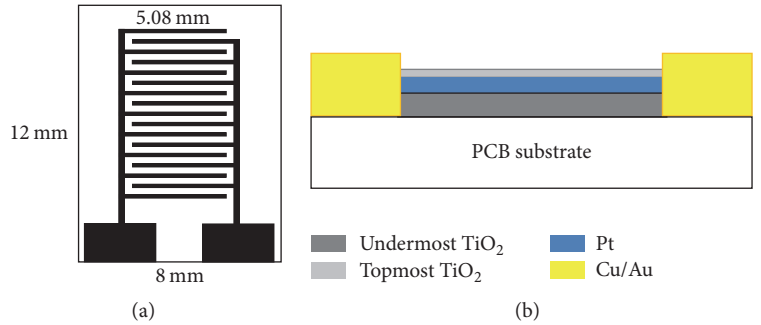

Figure 1: Schematic view of (a) PCB substrate and (b) TiO_2/Pt/TiO_2 sandwich nanostructures on the PCB substrate.

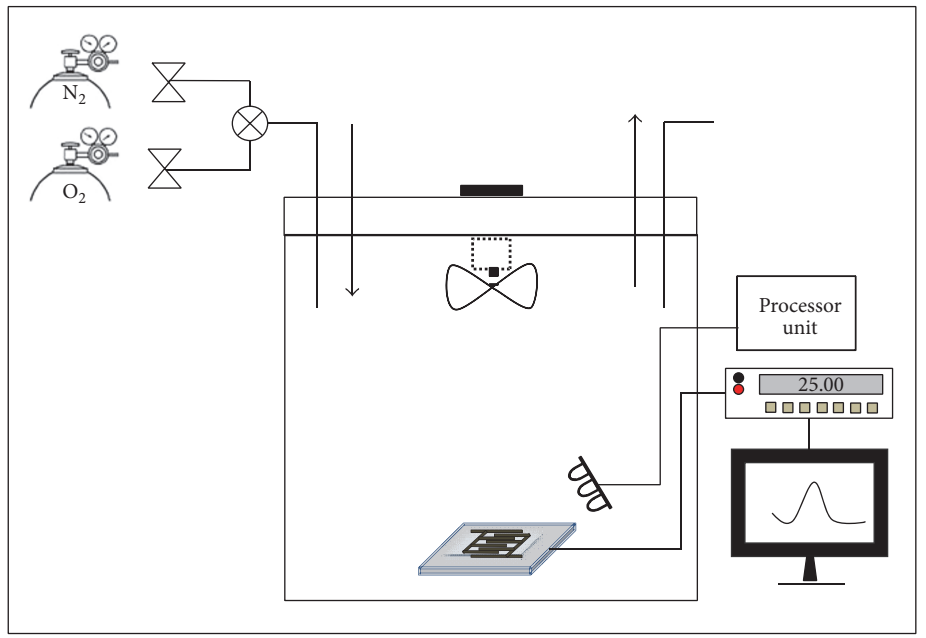

Figure 2: Schematic diagram of the system for gas sensor measurement.

sensor response and the time the sensor is back to its initial resistance, respectively.

3. Results and Discussions

3.1. Morphology, Structure, Composition, and Crystallinity of Sensing Materials. Figures 3(a) and 3(b) show SEM images of PCB substrate at low and high magnifications, respectively. The surface of the Cu/Au electrodes was relatively flat while the PCB substrate consists of a number of irregular-shaped pores with a diameter of approximately 50 μm and a relatively small pore with a diameter of approximately 3 μm embedded in a large pore. The pore structure of the PCB substrate provides a high surface area platform for sensing material deposition. Figures 3(c) and 3(d) show TEM images of the TiO_2/Pt/TiO_2 layers on Cu grid at low and high magnifications. Particles with different contrasts were uniformly dispersed in the matrix of sensing materials in which the bright and dark contrasts correspond to the TiO_2 and Pt particles, respectively. The high resolution of TEM image reflects the clear lattice fringes with an interplanar spacing of 0.23 nm corresponding to (111) plane of fcc Pt thus confirming formation of Pt nanoparticles in the TiO_2/Pt/TiO_2 layers. The size distribution of the Pt nanoparticles is 3-4 nm. Figure 3(e) shows the Auger depth profile of the TiO_2/Pt/TiO_2 layers on the SiO_2/Si substrate. Before sputtering, the peaks of titanium, oxygen, and platinum were found on the top-surface region. The composition ratio between Ti and O is 1 : 4. The nonstoichiometric Ti : O ratio in the top-surface region is due to air contamination, since the as-deposited film was exposed to the air before the AES measurement. After 15 min of sputtering, the peak of Pt appears apparently, showing a main content of the middle layer. After 50 min of sputtering, the Pt peaks disappeared and the peak of oxygen and titanium became strong again with the composition ratio between Ti and O is 1 : 2, indicating good stoichiometric TiO_2 film formation. The titanium and oxygen concentration is nearly constant in the whole film. However, spectra with a slope between the interfaces of each layer imply the interdiffusion of each sensing layer. It should be noted that the AES results

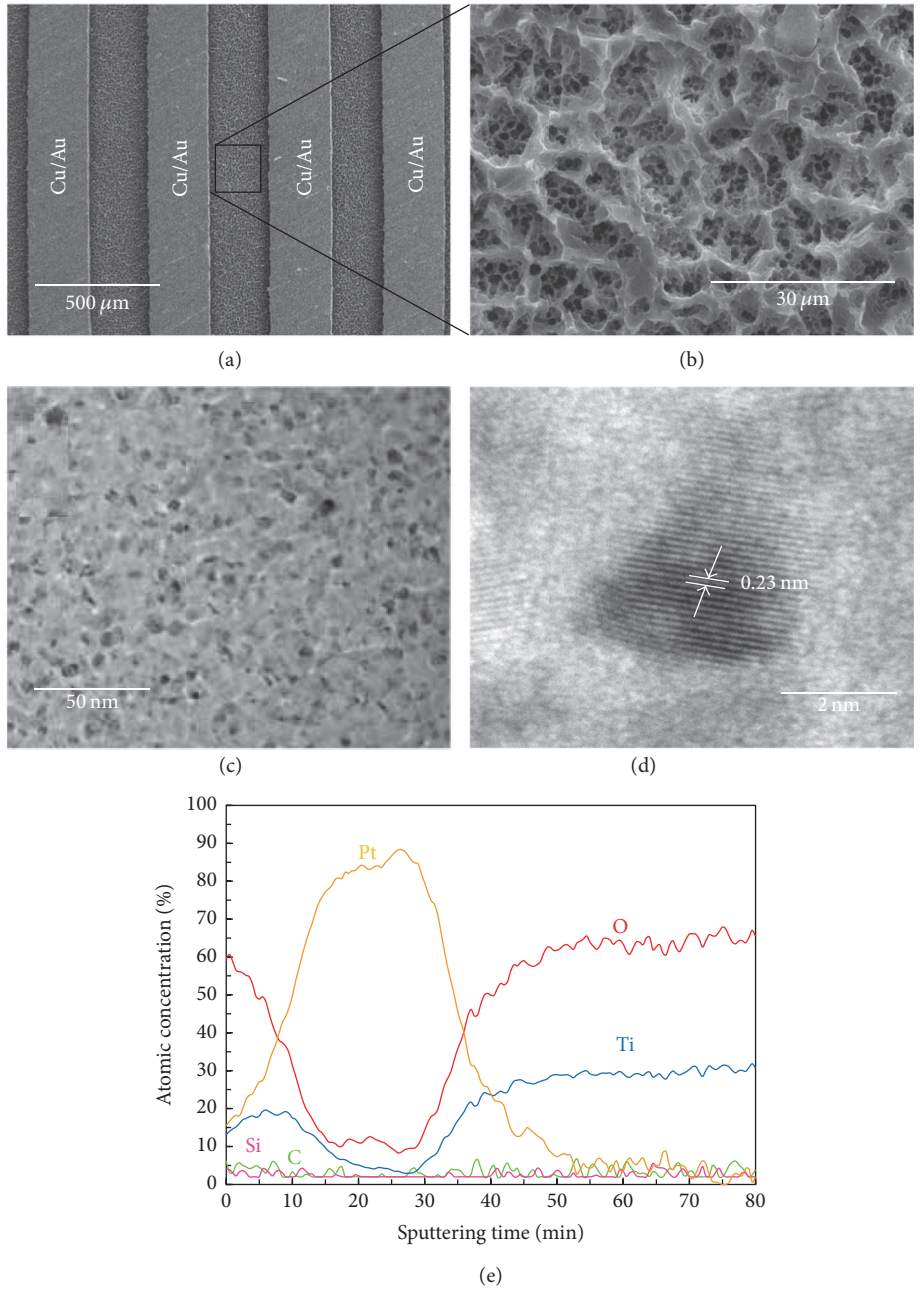

FIGURE 3: SEM images of PCB substrate at (a) low and (b) high magnifications, TEM images of the $TiO_2/Pt/TiO_2$ layers at (c) low and (d) high magnifications, and (e) Auger depth profile of the $TiO_2/Pt/TiO_2$ layers on the SiO_2/Si substrate.

obtained from the layers on the SiO_2/Si substrate cannot be directly referred to the layers on the PCB substrate because of the difference in surface morphology of each substrate.

3.2. Sensing Performance for Ethanol Vapor of Three Gas Sensors Based on Pt, TiO_2/Pt, and TiO_2/Pt/TiO_2. Figure 4(a) shows sensor responses of Pt, TiO_2/Pt, and $TiO_2/Pt/TiO_2$ to 100 ppm ethanol vapor. All of three sensors show an increase in resistance upon ethanol exposure and a decrease in resistance after switching to nitrogen atmosphere. Among three sensors, $TiO_2/Pt/TiO_2$ shows the highest sensor response, the fastest response time of 380 s, and the recovery time of 500 s. TiO_2/Pt shows a response with a small noise with a response time of 280 s and the recovery time of 600 s. Pt shows the less stable response and cannot recover to the initial resistance. Figure 4(b) shows a resistance of each sensor upon 100 ppm ethanol exposure to check a stability of a sensor for 30 days. The sensor response was recorded after ethanol exposure for 400 s. $TiO_2/Pt/TiO_2$ shows the most stable sensor response. TiO_2/Pt became stable after 5 days. However, the resistance of Pt gradually increased. This may due to the instability of Pt nanostructures under ambient, whereas the topmost and

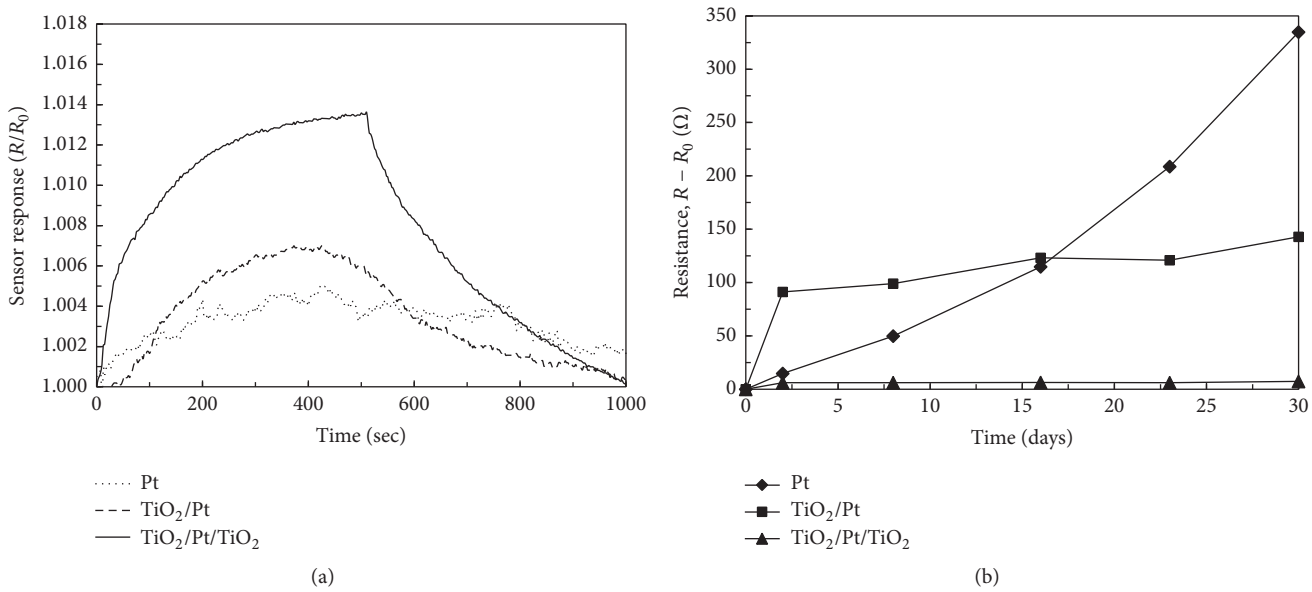

Figure 4: (a) Sensor responses of Pt, TiO_2/Pt, and TiO_2/Pt/TiO_2 to 100 ppm ethanol vapor and (b) resistance change of each sensor upon 100 ppm ethanol exposure.

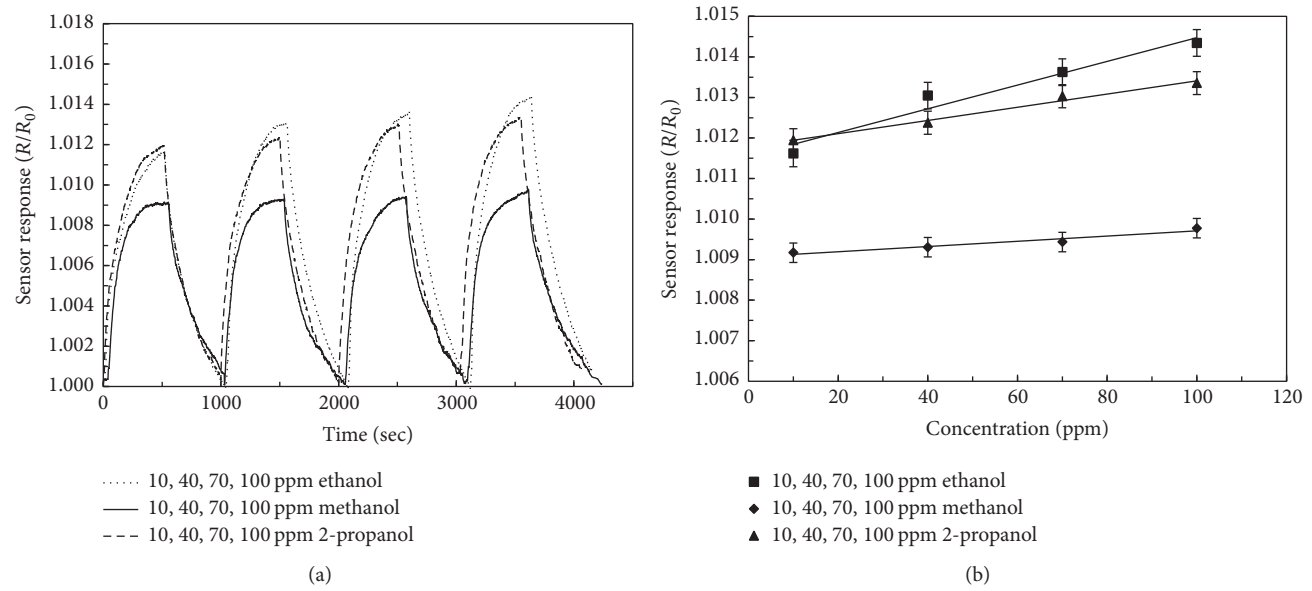

Figure 5: (a) Sensor responses to ethanol, methanol, and 2-propanol at a concentration range of 10 to 100 ppm and (b) relationship between vapor concentrations and sensor response.

undermost TiO_2 layers act as protective layer for Pt. This is similar to hydrogen sensing properties of single-walled carbon nanotubes protected by silicon oxide coating layer with palladium nanoparticle decoration [23, 24].

3.3. Sensing Performance of Gas Sensors of Ethanol, Methanol, and 2-Propanol Vapors. The sensing performances of TiO_2/Pt/TiO_2 of ethanol, methanol, and 2-propanol vapors were evaluated. The sensor was placed in the test chamber equipped with 365 nm UV light source. Figure 5(a) shows the sensor response to ethanol, methanol, and 2-propanol vapors at a concentration range of 10 to 100 ppm. The sensor response of TiO_2/Pt/TiO_2 increased upon 10 ppm ethanol exposure and decreased to the initial resistance after UV irradiation. The response time and recovery time were 285 s and 450 s, respectively. The sensor response increased gradually with the ethanol concentration. At ethanol 100 ppm, the response time and recovery time of sensor response to 100 ppm ethanol were 300 s and 450 s, respectively. Although the concentration of ethanol was up to 100 ppm, the recovery time was still in the same range of that of 10 ppm. The sensor responses to methanol and 2-propanol at a concentration range of 10 to

100 ppm show similar results to that of ethanol sensing but difference in response and recovery times. The sensor was successfully recovered by UV irradiation. This is attributed to the photocatalyst properties of TiO_2. The highly oxidizing effect of TiO_2 layers makes it suitable for decomposition of organic compounds [32]. The photocatalytic effect of TiO_2 can be used for cleaning surfaces of gas sensor that makes the recovery quick without using microheater. Figure 5(b) shows a relationship between vapor concentrations and sensor response, implying the linear relationship. Sensor response to ethanol showed the highest magnitude, while sensor response to methanol had the smallest magnitude.

The alcohol sensing mechanism of the TiO_2/Pt/TiO_2 has been discussed. First, the resistance change of TiO_2 upon alcohol exposure cannot explain the sensing mechanism of the TiO_2/Pt/TiO_2. This is supported by the fact that TiO_2 is an oxygen-deficient, intrinsically n-type material. Upon alcohol adsorption, free electron from alcohol oxidation reaction will be injected to TiO_2 layer and the conductivity of TiO_2 should be improved; however, the resistance of the TiO_2/Pt/TiO_2 increased. Second, the increase of Pt work function might explain the sensing mechanism. Although alcohol is generally regarded as an electron-donating reducing gas, it dissociates to CO and H_2 via oxidation reaction. It has been reported that CO molecule adsorbed on a Pt surface acts as a weak electron acceptor and induces an increase in the work function of Pt [35], resulting in an increase in resistance of the TiO_2/Pt/TiO_2.

In this work, the TiO_2/Pt/TiO_2 sandwich nanostructures were prepared by sputtering technique and were used as sensing material for ethanol, methanol, and 2-propanol detection in the sensor response results of the TiO_2/Pt/TiO_2 sandwich nanostructures to the recent researches on ethanol sensing which are mostly based on ZnO, SnO_2, and TiO_2 with various structures, such as nanoparticle, nanosphere, core-shell, nanotube and thin film, and various doping conditions [12–18]; it was found that the TiO_2/Pt/TiO_2 sandwich nanostructures show advantages in terms of 10 ppm level sensitivity, room-temperature operation, and stability. However, Ag@TiO_2 core-shell nanoparticles show the highest sensitivity down to 0.15 ppm ethanol with a fast response time and a fast recovery time but its fabrication process relies on wet process, which is time-consuming [15].

4. Conclusion

In this work, the TiO_2/Pt/TiO_2 sandwiched nanostructures were successfully prepared by an RF magnetron sputtering on PCB, SiO_2/Si substrate, and Cu grid. The formation of fcc Pt particle was investigated by TEM and the sandwich structure of the TiO_2/Pt/TiO_2 on the SiO_2/Si substrate was also confirmed by Auger electron spectroscopy with the interdiffusion of each layer. The alcohol sensors using the synthesized TiO_2/Pt/TiO_2 were also demonstrated at room temperature with a fast recovery by UV irradiation. The sensitivity and stability of the alcohol sensor based on the TiO_2/Pt/TiO_2 sandwich nanostructures revealed higher performance compared to the only Pt layer or the TiO_2/Pt structures. Furthermore, UV-assisted recovery by photocatalytic activity can improve the recovery time of the TiO_2/Pt/TiO_2 sandwich nanostructures. The highest response to ethanol vapor down to 10 ppm can be evaluated by using the optimum thicknesses of the TiO_2/Pt/TiO_2 sandwich nanostructure at 50 nm, 6 nm, and 6 nm, respectively. In addition, the TiO_2/Pt/TiO_2 sandwich nanostructure also shows an excellent sensing stability up to 30 days in which the topmost TiO_2 acts as a protective layer for Pt nanoparticles. The alcohol sensing mechanism could be explained by the increase of Pt work function during vapor exposure. The sensor was successfully recovered by photocatalytic reaction of TiO_2 layer under UV irradiation and the topmost TiO_2 also acts as protective layer for Pt.

Conflicts of Interest

The authors declare that they have no conflicts of interest.

Acknowledgments

This work has partially been supported by the National Nanotechnology Center (NANOTEC), NSTDA, Ministry of Science and Technology, Thailand, through its program of Center of Excellence Network. The authors also acknowledge the financial support from the Industrial Estate Authority of Thailand.

References

[1] A. A. Tomchenko, G. P. Harmer, B. T. Marquis, and J. W. Allen, "Semiconducting metal oxide sensor array for the selective detection of combustion gases," *Sensors and Actuators, B: Chemical*, vol. 93, no. 1-3, pp. 126–134, 2003.

[2] S. M. Kanan, O. M. El-Kadri, I. A. Abu-Yousef, and M. C. Kanan, "Semiconducting metal oxide based sensors for selective gas pollutant detection," *Sensors*, vol. 9, no. 10, pp. 8158–8196, 2009.

[3] L. Filipovic and S. Selberherr, "Performance and stress analysis of metal oxide films for CMOS-integrated gas sensors," *Sensors (Switzerland)*, vol. 15, no. 4, pp. 7206–7227, 2015.

[4] J. Huang and Q. Wan, "Gas sensors based on semiconducting metal oxide one-dimensional nanostructures," *Sensors*, vol. 9, no. 12, pp. 9903–9924, 2009.

[5] T. Konduru, G. C. Rains, and C. Li, "A customized metal oxide semiconductor-based gas sensor array for onion quality evaluation: System development and characterization," *Sensors (Switzerland)*, vol. 15, no. 1, pp. 1252–1273, 2015.

[6] Y.-F. Sun, S.-B. Liu, F.-L. Meng et al., "Metal oxide nanostructures and their gas sensing properties: a review," *Sensors*, vol. 12, no. 3, pp. 2610–2631, 2012.

[7] C. Wang, L. Yin, L. Zhang, D. Xiang, and R. Gao, "Metal oxide gas sensors: sensitivity and influencing factors," *Sensors*, vol. 10, no. 3, pp. 2088–2106, 2010.

[8] E. Comini, "Metal oxide nano-crystals for gas sensing," *Analytica Chimica Acta*, vol. 568, no. 1-2, pp. 28–40, 2006.

[9] E. Comini, L. Yubao, Y. Brando, and G. Sberveglieri, "Gas sensing properties of MoO3 nanorods to CO and CH 3OH," *Chemical Physics Letters*, vol. 407, no. 4-6, pp. 368–371, 2005.

[10] E. Comini and G. Sberveglieri, "Metal oxide nanowires as chemical sensors," *Materials Today*, vol. 13, no. 7-8, pp. 36–44, 2010.

[11] N. G. Cho, H.-S. Woo, J.-H. Lee, and I.-D. Kim, "Thin-walled NiO tubes functionalized with catalytic Pt for highly selective C2H5OH sensors using electrospun fibers as a sacrificial template," *Chemical Communications*, vol. 47, no. 40, pp. 11300–11302, 2011.

[12] A. Tamvakos, D. Calestani, D. Tamvakos, R. Mosca, D. Pullini, and A. Pruna, "Effect of grain-size on the ethanol vapor sensing properties of room-temperature sputtered ZnO thin films," *Microchimica Acta*, vol. 182, no. 11-12, pp. 1991–1999, 2015.

[13] S. M. Chou, L. G. Teoh, W. H. Lai, Y. H. Su, and M. H. Hon, "ZnO:Al thin film gas sensor for detection of ethanol vapor," *Sensors*, vol. 6, no. 10, pp. 1420–1427, 2006.

[14] J. Liu, T. Wang, B. Wang et al., "Highly sensitive and low detection limit of ethanol gas sensor based on hollow ZnO/SnO2 spheres composite material," *Sensors and Actuators, B: Chemical*, vol. 245, pp. 551–559, 2017.

[15] Z. Zhu, C.-T. Kao, and R.-J. Wu, "A highly sensitive ethanol sensor based on Ag@TiO2 nanoparticles at room temperature," *Applied Surface Science*, vol. 320, pp. 348–355, 2014.

[16] A. Hazra, K. Dutta, B. Bhowmik, P. P. Chattopadhyay, and P. Bhattacharyya, "Room temperature alcohol sensing by oxygen vacancy controlled TiO 2 nanotube array," *Applied Physics Letters*, vol. 105, no. 8, Article ID 081604, 2014.

[17] K. P. Priyanka, S. C. Vattappalam, S. Sankararaman, K. M. Balakrishna, and T. Varghese, "High-performance ethanol gas sensor using TiO2 nanostructures," *The European Physical Journal Plus*, vol. 132, no. 7, 2017.

[18] J. Zhang, P. Tang, T. Liu, Y. Feng, C. Blackman, and D. Li, "Facile synthesis of mesoporous hierarchical Co," *Journal of Materials Chemistry A*, vol. 5, no. 21, pp. 10387–10397, 2017.

[19] J. Kong, N. R. Franklin, C. Zhou et al., "Nanotube molecular wires as chemical sensors," *Science*, vol. 287, no. 5453, pp. 622–625, 2000.

[20] W. Wongwiriyapan, S.-I. Honda, H. Konishi et al., "Single-walled carbon nanotube thin-film sensor for ultrasensitive gas detection," *Japanese Journal of Applied Physics, Part 2: Letters*, vol. 44, no. 16-19, pp. L482–L484, 2005.

[21] W. Wongwiriyapan, S. Inoue, T. Ito et al., "Highly sensitive detection of carbon monoxide at room temperature using platinum-decorated single-walled carbon nanotubes," *Applied Physics Express*, vol. 1, no. 1, 2008.

[22] A. Star, V. Joshi, S. Skarupo, D. Thomas, and J.-C. P. Gabriel, "Gas sensor array based on metal-decorated carbon nanotubes," *Journal of Physical Chemistry B*, vol. 110, no. 42, pp. 21014–21020, 2006.

[23] W. Wongwiriyapan, S. Inoue, Y. Okabayashi et al., "Highly stable and sensitive gas sensor based on single-walled carbon nanotubes protected by metal-oxide coating layer," *Applied Physics Express*, vol. 2, no. 9, Article ID 095008, 2009.

[24] W. Wongwiriyapan, Y. Okabayashi, S. Minami et al., "Hydrogen sensing properties of protective-layer-coated single-walled carbon nanotubes with palladium nanoparticle decoration," *Nanotechnology*, vol. 22, no. 5, Article ID 055501, 2011.

[25] R. J. Chen, N. R. Franklin, J. Kong et al., "Molecular photodesorption from single-walled carbon nanotubes," *Applied Physics Letters*, vol. 79, no. 14, pp. 2258–2260, 2001.

[26] V. Dua, S. P. Surwade, S. Ammu et al., "All-organic vapor sensor using inkjet-printed reduced graphene oxide," *Angewandte Chemie*, vol. 49, no. 12, pp. 2154–2157, 2010.

[27] D. Buso, M. Post, C. Cantalini, P. Mulvaney, and A. Martucci, "Gold nanoparticle-doped TiO2 semiconductor thin films: gas sensing properties," *Advanced Functional Materials*, vol. 18, no. 23, pp. 3843–3849, 2008.

[28] T. Tesfamichael, A. Ponzoni, M. Ahsan, and G. Faglia, "Gas sensing characteristics of Fe-doped tungsten oxide thin films," *Sensors and Actuators, B: Chemical*, vol. 168, pp. 345–353, 2012.

[29] L. Zhu, D. Zhang, Y. Wang et al., "Xylene gas sensor based on Ni doped TiO2 bowl-like submicron particles with enhanced sensing performance," *RSC Advances*, vol. 5, no. 36, pp. 28105–28110, 2015.

[30] L. A. Patil, D. N. Suryawanshi, I. G. Pathan, and D. M. Patil, "Nickel doped spray pyrolyzed nanostructured TiO2 thin films for LPG gas sensing," *Sensors and Actuators, B: Chemical*, vol. 176, pp. 514–521, 2013.

[31] A. M. Ruiz, A. Cornet, K. Shimanoe, J. R. Morante, and N. Yamazoe, "Transition metals (Co, Cu) as additives on hydrothermally treated Tio2 for gas sensing," *Sensors and Actuators, B: Chemical*, vol. 109, no. 1, pp. 7–12, 2005.

[32] X. Cheng, Y. Xu, S. Gao, H. Zhao, and L. Huo, "Ag nanoparticles modified TiO2 spherical heterostructures with enhanced gas-sensing performance," *Sensors and Actuators, B: Chemical*, vol. 155, no. 2, pp. 716–721, 2011.

[33] A. Ruiz, J. Arbiol, A. Cirera, A. Cornet, and J. R. Morante, "Surface activation by Pt-nanoclusters on titania for gas sensing applications," *Materials Science and Engineering C*, vol. 19, no. 1-2, pp. 105–109, 2002.

[34] M. Zhang, Z. Yuan, J. Song, and C. Zheng, "Improvement and mechanism for the fast response of a Pt/TiO2 gas sensor," *Sensors and Actuators, B: Chemical*, vol. 148, no. 1, pp. 87–92, 2010.

[35] S. Nettesheim, A. Von Oertzen, H. H. Rotermund, and G. Ertl, "Reaction diffusion patterns in the catalytic CO-oxidation on Pt(110): front propagation and spiral waves," *The Journal of Chemical Physics*, vol. 98, no. 12, pp. 9977–9985, 1993.